Density functional theory study of ZnX (X=O, S, Se, Te) under uniaxial strain

S. K. Yadav, T. Sadowski, and R. Ramprasad*
Chemical, Materials, and Biomolecular Engineering, Institute of Materials Science, University of Connecticut, Storrs, Connecticut 06269, USA

(Received 17 November 2009; revised manuscript received 16 March 2010; published 20 April 2010)

We present a first principles density functional theory based study of the impact of uniaxial strain on the structural and electronic properties of bulk ZnX (X=O, S, Se, Te) in the wurtzite and zinc blende phases. The strain axis was chosen to be along the [0001] and [111] directions, respectively, for the wurtzite and zinc blende systems. For large uniaxial compressive strains, all systems undergo a transition from the equilibrium wurtzite or zinc blende phases to a pseudographitic phase. Simultaneously, the band gap of the systems gradually drops to a small or zero value. Under large uniaxial tensile strains, all systems tend to form individual stoichiometric ZnX layers, also with small band gap values relative to the corresponding equilibrium ones. Although the range of strains considered here is enormous, appreciable changes (i.e., reductions) of the band gap may be accomplished for modest and realistic strains achievable in nanowires.

DOI: 10.1103/PhysRevB.81.144120 PACS number(s): 71.30.+h

I. INTRODUCTION

It is well-known that structural phase transformations in materials systems may be induced through application of appropriate stresses.[1] An interesting example of such an occurrence in confined geometries has recently been reported for ZnO nanowires, studied using density functional theory (DFT) based computations.[2–5] It was determined that a critical uniaxial compressive stress along the nanowire [0001] axis results in the transformation of the system from the equilibrium wurtzite to a pseudographitic structure. Concomitant with this phase transformation is a change in electronic structure which reduces the band gap.[4]

Such strain-induced variations in structural and electronic properties are not only intriguing, but are also attractive technologically. For instance, the environmentally benign Zn-based semiconductors have large band gap, but reductions in their band gap will make them appropriate for photovoltaic applications. In order to better understand potentially useful strain-induced structural and electronic property modulations of the type referred to above, we have undertaken a comprehensive DFT study of bulk ZnX (X=O, S, Se, Te) under uniaxial strain.

ZnX systems in both wurtzite (W) and zinc blende (Z) phases were considered. In order to mimic situations encountered in nanowire geometries, the ZnX systems were subjected to uniaxial strain in the following manner: the W phases were strained along the [0001] (or the $\boldsymbol{c}$) axis, and the Z phases along the [111] direction (which is equivalent to the W [0001] direction). These chosen strain axes are the most preferred nanowire growth directions along which strains may be present or imposed.

Under large uniaxial compression, we show here rigorously that both the W and Z phases display a tendency to "graphitize," i.e., the Zn (or X) atom becomes coplanar with the three X (or Zn) atoms below (above), resulting in honeycomblike layers normal to the strain axes (see Fig. 1). We refer to this phase as pseudographitic or graphitelike (rather than graphitic) for two reasons: (1) the relationship between adjacent layers is different from that in graphite, and (2) the coordination number of Zn and X atoms may be greater than 3 due to the proximity of adjacent layers (similar to the trend anticipated for Group 14 elements).[6] The W and Z phases, along with the pseudographitic versions of the W and Z phases (henceforth referred to as W-G and Z-G, respectively) are shown in Fig. 1. Progressively increasing tensile strains leads to the formation of individual stoichiometric ZnX layers. Drastic reductions in band gap values accompany the structural changes under both compression and tension.

In addition to the prediction of strain-induced structural transformations (including transformation stresses) and band gap modulations, an important outcome of this work is the universality of such behaviors within the ZnX family of wide

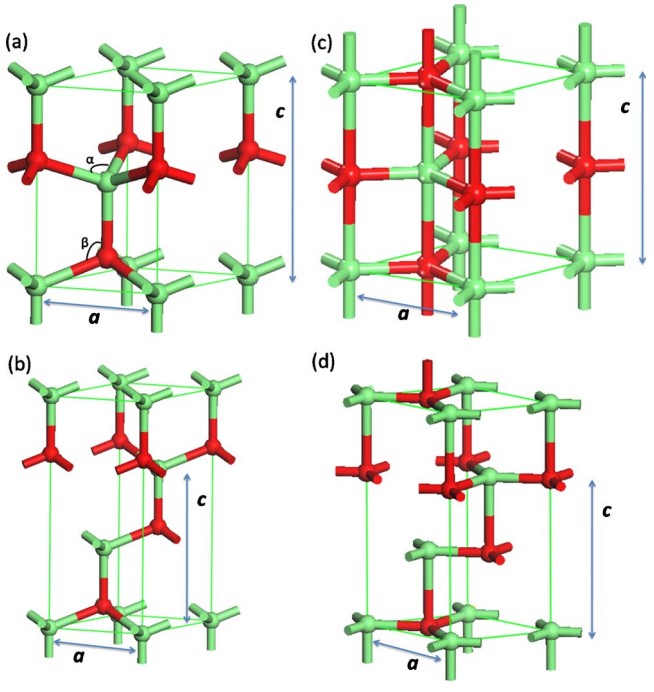

FIG. 1. (Color online) Phases of ZnX: (a) Wurtzite (w), (b) Zinc blende (z), (c) Graphitelike phase derived from wurtzite (W-G), and (d) Graphitelike phase derived from zinc blende (Z-G).

TABLE I. Calculated equilibrium lattice parameters, in Å, of Zn*X* in the wurtzite (W) and zinc blende (Z) phases, compared with experiments. Also listed is the energy per Zn*X* pair (*E*) in meV, with respect to the W phase for each system.

		This work			Expt.	
System	Phase	*E*	***a***	***c***	***a***	***c***
ZnO	W	0	3.29	5.28	3.24	5.20
	Z	55	4.60			
ZnS	W	0	3.85	6.29	3.82	6.26
	Z	−6	5.45		5.41	
ZnSe	W	0	4.05	6.62	4.00	6.54
	Z	−9	5.73		5.67	
ZnTe	W	0	4.36	7.14	4.27	6.99
	Z	−12	6.16		6.10	

band gap semiconductors. We also note that the Zn*X* series displays interesting chemical trends. For instance, increasing values of the anion (*X*) atomic number correlate to greater sensitivity of the band gap variation with strain.

This article is organized as follows. Details of the calculations along with descriptions of the structural models are provided in Sec. II. Our results concerning structural changes, transformation stresses, and electronic structure modulations due to strain are described in detail in Sec. III. We discuss the implications of our findings in Sec. IV, before concluding with a summary in Sec. V.

II. METHODS AND MODELS

Our DFT calculations were performed using the Vienna *ab initio* simulation package (VASP) (Ref. 7) with the PW91 generalized gradient approximation,[8] projector-augmented wave (PAW) (Ref. 9) pseudopotentials and a cut-off energy of 495 eV for the plane wave expansion of the wave functions. A Monkhorst-Pack *k*-point mesh of at least $5\times5\times5$ was required to obtain well-converged results. Structural and energetic results for strainfree bulk Zn*X* systems determined using these approximations and parameters are listed in Table I. The lattice parameters (***a*** and ***c*** for the W phase, and ***a*** for the Z phase) obtained here are in reasonable agreement with available experimental data.[10,11] Moreover, the predicted equilibrium phase is W for ZnO and Z for ZnS, ZnSe, and ZnTe, again in agreement with prior work.[11]

Calculations involving strain required just the primitive unit cell containing two Zn*X* pairs for the W phases [Fig. 1(a)], but unit cells containing three Zn*X* pairs were required in the case of the Z phases [Fig. 1(b)]. For ease of comparison, we define the ***c*** of the Z phase to be 2/3 of the height of the unit cell shown in Fig. 1(b), so that this ***c*** is commensurate with that of the W phase. In anticipation of the tendency for graphitization, calculations in which the symmetry of the system was constrained to be in the W-G or Z-G phases were also performed, using the unit cells shown in Figs. 1(c) and 1(d), respectively. In all calculations involving strain, ***c*** was fixed at a specific value, and the optimal value of ***a*** corresponding to each fixed ***c*** value was determined. All such calculations involved optimization of the atomic positions such that each component of the force on every atom was smaller than 0.02 eV/Å.

III. RESULTS

A. Structural transformations

Figure 2(a) shows variation of ***a*** with ***c*** for the W and Z phases, with the inset showing the corresponding variation of the relative change in the volume of the unit cell with uniaxial strain. Interestingly, while the ***a*** and the volume change are roughly equivalent for the W and the Z phases for most of the strain range considered, the volume change in the W phase appears to saturate at about −6% beyond compressive strains of about −10%, while the Z phase continues to show decreases in volume beyond this strain.

The most dramatic feature of the structural changes with respect to uniaxial compression is the transformation of the systems from structures that display sp^3 hybridization to ones that display graphitelike features. This transformation is evident from Fig. 2(b), which portrays the variation of the two inequivalent *X*-Zn-*X* bond angles [α and β, defined in Fig. 1(a)] with ***c*** for the W phase. While α and β are both 109.5° close to equilibrium (characteristic of sp^3 hybridization in the W phase), they gradually approach limiting values of 120° and 90°, respectively. The inset of Fig. 2(b) shows that for uniaxial compressive strains greater than about 15%, transformation to the graphitelike phase is complete.

For large tensile uniaxial strains, α and β saturate at 114° and 104°, respectively. Thus, in the limit of large ***c***, individual stoichiometric Zn*X* layers are formed, but the Zn and *X* atoms are not in the same plane. Although the range of strains considered here may be viewed as being unrealistically large, we note that strains as high as 15% have been observed before fracture in ZnO nanowires with diameters of about 200 nm.[12] Also, large strains without the creation of extended defects may be achieved in epitaxial core-shell heterostructure nanowires (through lattice mismatches).[13,14]

B. Transformation stresses

In order to determine the stresses at which the W or Z phase may be expected to transform to the W-G or Z-G

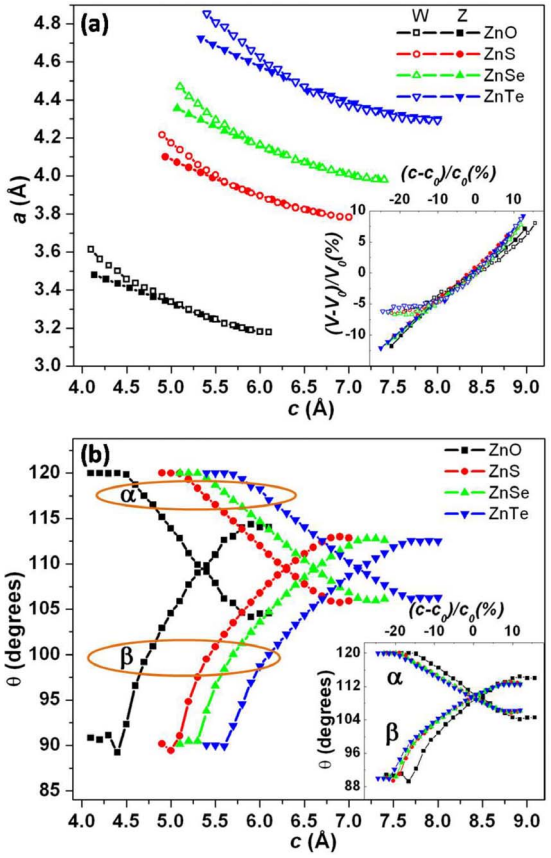

FIG. 2. (Color online) (a) Variation of a with c. Inset shows the corresponding variation of the change in the volume of the unit cell with respect to the change in the c, with respect to the corresponding equilibrium values c_0 and V_0. (b) Variation of the angles α and β [defined in Fig. 1(a)] with c in the W phase. The ovals group together curves corresponding to the same angle (α or β). Inset shows the same data as the main plot, but in terms of the variation of the angles with change in c.

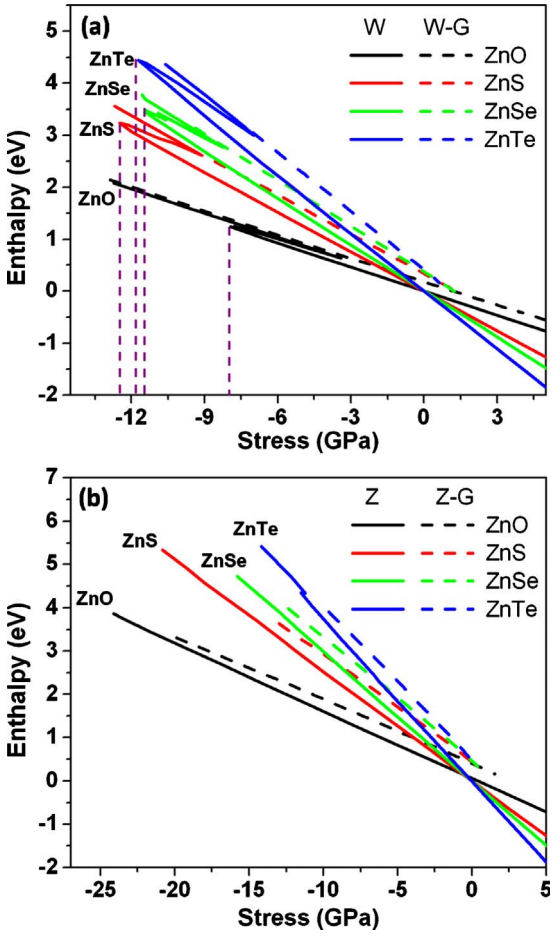

FIG. 3. (Color online) Enthalpy per ZnX unit as a function of uniaxial stress along the c axis for (a) the W and W-G phases, and for (b) the Z and Z-G phases. Positive (negative) values of stresses represent tension (compression).

phase, the enthalpy per ZnX unit, H, of each of the phases considered was determined as a function of the uniaxial stress, using the relation: $H=E-\sigma_z V$, where E, σ_z, and V are, respectively, the energy per ZnX unit, the uniaxial stress along the c axis, and the volume per ZnX unit. Figure 3 displays our results. Focusing first on the W→W-G transformation [Fig. 3(a)], it is evident that under tensile stresses (positive σ_z values), the W phases are all more stable than the W-G phases. However, under compressive stresses, all ZnX W phases clearly display instabilities to the transformation to the corresponding W-G phases. The instabilities are characterized by "kinks" when the W enthalpy curves abruptly become coincident with the W-G enthalpy curves. The locations of the kinks are indicated using vertical dotted lines in Fig. 3(a). The compressive stresses corresponding to the kinks (taken to be the W→W-G transformation stresses) are estimated to be about 8, 12.5, 11.5, and 11.8 GPa, respectively, for ZnO, ZnS, ZnSe, and ZnTe.

In contrast to the W→W-G transformation, the Z→Z-G transition [Fig. 3(b)] appears to occur much more smoothly, and asymptotically, although the presence of faint kinks can be seen for ZnTe. We are thus unable to provide actual transformation stress values for the Z→Z-G transitions.

C. Electronic structure changes

The variation of the band gap with the value of c is shown in Fig. 4. We note that although DFT underestimates the absolute value of the band gap, trends in band gap value changes are well predicted. For instance, although the band gap of ZnO is predicted to be 0.86 eV, considerably underestimated with respect to the experimental value of 3.37 eV, the first derivative of the band gap with respect to uniaxial strain along the c axis is determined here to be 0.02 eV for the equilibrium W phase, identical to the corresponding experimental value.[15] Moreover, DFT and the more sophisticated GW theory usually agree on pressure coefficients of band gap.[16] Also, the specific choice of the exchange-correlation functional appears not to change the trends in the variation of the band gap values. Figure 4(a), for instance, shows band gap values calculated using both the GGA and the local density approximation (LDA) as a function of c for the W phase. The qualitative similarity between the LDA and GGA predictions is manifest.

Thus, in addition to the actual band gap values, we also show percentage changes of the predicted GGA band gap as

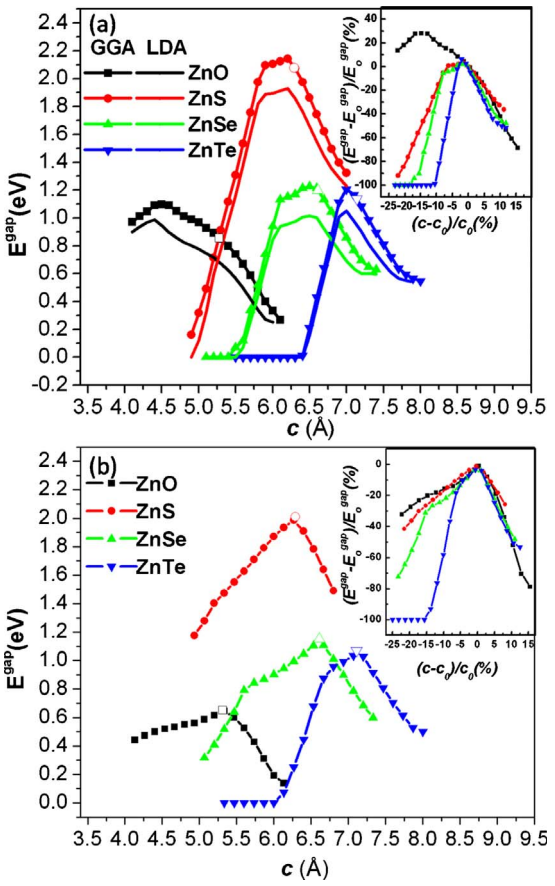

FIG. 4. (Color online) Band gap (E^{gap}) as a function of $\boldsymbol{c}$ for (a) the W phase, using the LDA (without symbols) and the GGA (with symbol), and (b) the Z phase using the GGA. The band gap value at equilibrium (E_0^{gap}) is indicated for each case using open symbols. Insets show the corresponding relative change in the GGA band gap value with uniaxial strain.

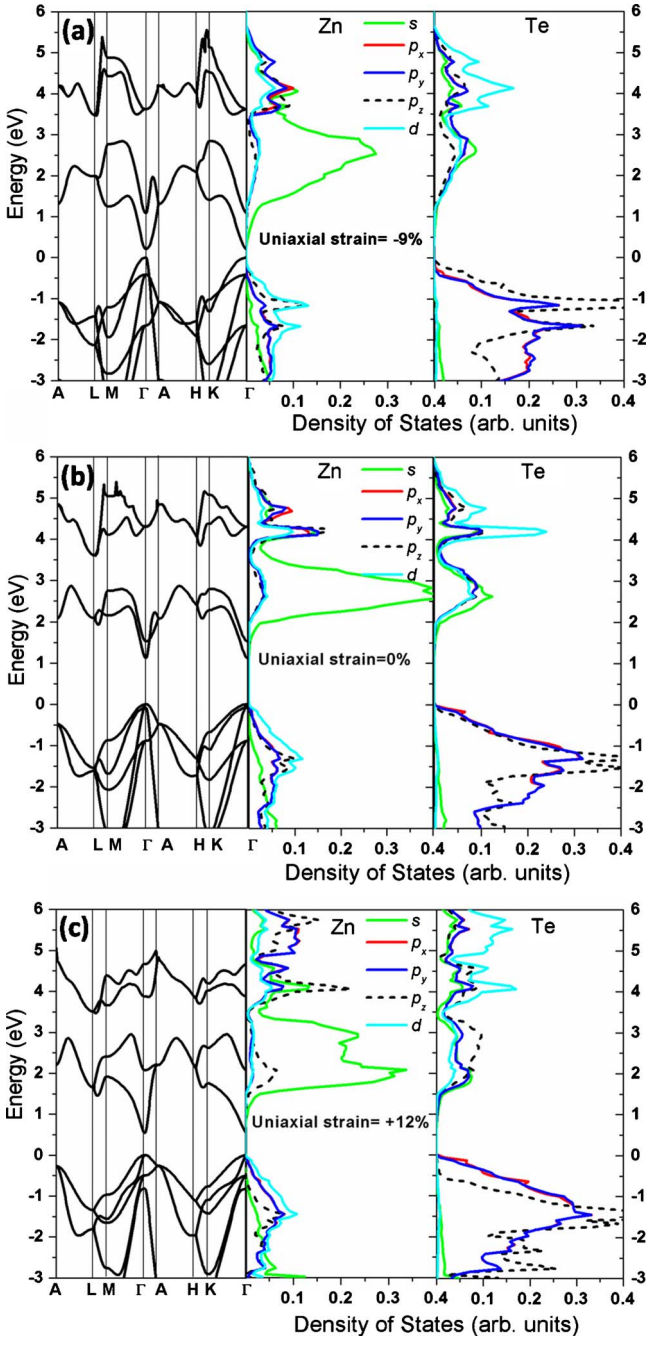

FIG. 5. (Color online) Band structure and density of states (DOS) of ZnTe at uniaxial strains of −9% (a), 0% (b), and +12% (c). The left panel of each plot displays the band structure, the middle panel shows the DOS arising from the Zn s, p_x, p_y, p_z, and d orbitals, and the right panel displays the DOS due to the Te s, p_x, p_y, and p_z orbitals.

a function of strain in the insets of Fig. 4. Several interesting observations can be made: (1) in all W phase cases [Fig. 4(a)], uniaxial stretching along the $\boldsymbol{c}$ axis results in a decrease in the band gap. Upon uniaxial compression, the band gap initially increases slightly (consistent with prior experimental and theoretical work)[15,17] goes through a maximum, eventually decreases and approaches zero. The initial increase in the band gap under compression is the natural result of bonding and antibonding orbitals becoming more stabilized and destabilized, respectively. (2) In the case of the Z phases [Fig. 4(b)], the maximum value of the band gap occurs at equilibrium (i.e., under strainfree situations). Both uniaxial tension and compression result in a decrease in the band gap value for all 4 ZnX systems studied. (3) In both W and Z phases, as can be seen from the insets of Fig. 4, the behavior of the change of the band gap with respect to strain is identical under uniaxial tension.

We note however that the rate at which the change in the band gap value drops under compression to −100% (corresponding to a zero band gap) depends on the identity of the X anion. For instance, ~10% uniaxial compression in the case of ZnTe in the W phase makes it metallic, whereas in the case of ZnO, a compression larger than 20% may be required to make its band gap vanish. This direct correlation between anion atomic number and sensitivity to uniaxial strain levels is reminiscent of a similar correlation between anion size and the pressure coefficient of the band gap[17] (identified earlier to be due to enhanced $s-s$ and $p-p$ coupling between cation and anion atoms).

To better understand the factors underlying the above mentioned band gap variations, we briefly consider details of

the band structure. Figure 5 shows the band structure and density of states (DOS) of ZnTe in the W phase at uniaxial strains of −9%, 0%, and +12%. We note that the band structure at equilibrium (i.e., at 0% strain) computed here is in excellent agreement with prior work.[18–20] At equilibrium, as can be seen from the DOS plots of Fig. 5(b), the Zn d orbitals and the Te p orbitals contribute the most to the valence band maximum states, while the Zn s orbitals dominate the conduction band minimum states. The significant overlap of the Te p_x, p_y, and p_z orbital DOS close to the valence band maximum is evidence of the sp^3 hybridization at work (at equilibrium). As can be seen in Figs. 5(a) and 5(c), the band gap decrease at uniaxial strains of −9% or +12% is accompanied by a reduction in this overlap: the Te p_z orbital DOS splits away from the Te p_x and p_y orbital DOS curves. Qualitatively similar behavior was seen in the case of the other systems as well, although the amount of the $s-s$ and $p-p$ Zn-X overlap (at the conduction and valence bands, respectively) progressively decreases for decreasing anion atomic number. The electronic structure variation with strain is thus consistent with the corresponding structural variation discussed earlier (Fig. 2).

IV. IMPLICATIONS

Geometric and electronic structure changes accompanying uniaxial strain appear to be somewhat universal in ZnX systems. The stabilization of the W-G and Z-G phases with respect to the W and Z phases in a bulk environment is not as dramatic as in ultrathin ZnO nanowires.[2–5] Still, both compressive and tensile strains of the right amount may result in substantial *decreases* in the band gap with respect to the corresponding equilibrium values, with this effect presumably heightened in systems with decreased dimensionality. This may explain the recent prediction that *both* the core and shell region materials (under tension and compression, respectively) in ZnO/ZnS and ZnO/ZnTe core/shell wurtzite [0001] nanowires display a decrease in band gap values relative to their equilibrium bulk values.[10] Core/shell nanowires thus offer promising geometric situations that may be exploited for band gap engineering.[10,21] Another situation where a controlled amount of strain may be imposed is in ultrathin pseudomorphically grown ZnX films on appropriately lattice-mismatched substrates. Such approaches may open up opportunities for Zn-based photovoltaic systems.

V. SUMMARY

In summary, we have studied the physical and electronic properties of bulk ZnX (X=O, S, Se, Te) systems over a wide range of uniaxial strains along the wurtzite [0001] or the zinc blende [111] axes. In particular, we have correlated structural changes accompanying uniaxial strains with electronic structure changes. We find that for large values of compressive strains, all ZnX systems considered transform to a pseudographitic phase displaying very small band gaps. Tensile strain leads to layered structures and small band gaps. Although the range of strains considered here is large, these computations have identified opportunities for engineering the band gap of Zn-based semiconductors (e.g., decreasing it to the visible spectrum range) through strain levels achievable in core/shell nanowires and epitaxial films on lattice-mismatched substrates.

ACKNOWLEDGMENTS

Financial support of this work through a grant from the National Science Foundation (NSF) and computational support through a NSF Teragrid Resource Allocation are acknowledged. Helpful discussions with Roald Hoffmann are also gratefully acknowledged.

*rampi@ims.uconn.edu

[1] W. B. Holzapfel, Rep. Prog. Phys. **59**, 29 (1996).
[2] A. J. Kulkarni, M. Zhou, K. Sarasamak, and S. Limpijumnong, Phys. Rev. Lett. **97**, 105502 (2006).
[3] B. Wang, J. Zhao, J. Jia, D. Shi, J. Wan, and G. Wang, Appl. Phys. Lett. **93**, 021918 (2008).
[4] Y. Zhang, Y.-H. Wen, J.-C. Zheng, and Z.-Z. Zhuc, Appl. Phys. Lett. **94**, 113114 (2009).
[5] L. Zhang and H. Huang, Appl. Phys. Lett. **90**, 023115 (2007).
[6] X.-D. Wen, T. J. Cahill, and R. Hoffmann (unpublished).
[7] G. Kresse and J. Furthmuller, Phys. Rev. B **54**, 11169 (1996).
[8] J. P. Perdew, J. A. Chevary, S. H. Vosko, K. A. Jackson, M. R. Pederson, D. J. Singh, and C. Fiolhais, Phys. Rev. B **46**, 6671 (1992).
[9] P. E. Blöchl, Phys. Rev. B **50**, 17953 (1994).
[10] J. Schrier, D. O. Demchenko, L.-W. Wang, and A. P. Alivisatos, Nano Lett. **7**, 2377 (2007).
[11] C.-Y. Yeh, Z. W. Lu, S. Froyen, and A. Zunger, Phys. Rev. B **46**, 10086 (1992).
[12] A. V. Desai and M. A. Haque, Sens. Actuators, A **134**, 169 (2007).
[13] L. J. Lauhon, M. S. Gudiksen, D. Wang, and C. M. Lieber, Nature (London) **420**, 57 (2002).
[14] E. Ertekin, P. A. Greany, D. C. Chrzan, and T. D. Sands, J. Appl. Phys. **97**, 114325 (2005).
[15] R. Ghosh, J. Basak, and S. Fujihara, J. Appl. Phys. **96**, 2689 (2004).
[16] X. Zhu, S. Fahy, and S. G. Louie, Phys. Rev. B **39**, 7840 (1989).
[17] S.-H. Wei and A. Zunger, Phys. Rev. B **60**, 5404 (1999).
[18] O. Zakharov, A. Rubio, X. Blase, M. L. Cohen, and S. G. Louie, Phys. Rev. B **50**, 10780 (1994).
[19] P. Schröer, P. Krüger, and J. Pollmann, Phys. Rev. B **47**, 6971 (1993).
[20] A. Kobayashi, O. F. Sankey, S. M. Volz, and J. D. Dow, Phys. Rev. B **28**, 935 (1983).
[21] T. Sadowski and R. Ramprasad, J. Phys. Chem. C **114**, 1773 (2010).